



Electronic instability during vortex motion in cuprate superconductors

Regime of low and high magnetic fields

S.G. Doettinger ^a, R.P. Huebener ^{a,*}, A. Kühle ^b

^a *Physikalisches Institut, Lehrstuhl Experimentalphysik II, University of Tübingen, Morgenstelle 14, D-72076 Tübingen, Germany*

^b *Physics Department, Technical University of Denmark, DK-2800 Lyngby, Denmark*

Received 2 June 1995

Abstract

The critical velocity v_φ^* associated with the electronic instability predicted by Larkin and Ovchinnikov displays a cross-over effect from magnetic-field independent behavior at high fields to the proportionality $v_\varphi^* \sim B^{-1/2}$ at low fields. This low-field behavior results from the fact that v_φ^* multiplied with the inelastic quasiparticle scattering time τ_{in} must reach at least the intervortex distance, thereby ensuring spatial homogeneity of the nonequilibrium quasiparticle distribution. At high magnetic fields the flux-flow instability becomes unobservable due to the onset of fluctuation effects contributing to the resistivity.

1. Introduction

Recently we have reported on the first observation of an electronic instability at high flux-flow velocities in high- T_c superconducting films [1,2]. This instability manifests itself as a distinct break in the voltage–current characteristic (VIC) and is due to the nonequilibrium distribution of the quasiparticles in the presence of an electric field of sufficient magnitude. This highly nonlinear behavior has been predicted about 20 years ago by Larkin and Ovchinnikov (LO) [3], based on Eliashberg's ideas on the nonequilibrium effects in superconductors. The essential physics is as follows. As a result of the electric field generated from current-induced vortex motion the distribution of the quasiparticles is shifted

to higher energies compared to the equilibrium distribution. As a consequence, quasiparticles leave the potential well of the vortex core, the vortex core shrinks, viscous damping of the vortex motion is reduced, and the VIC shows upwards curvature. According to LO [3] the viscous-damping coefficient η at vortex velocity v_φ is

$$\eta(v_\varphi) = \frac{\eta(0)}{1 + \left(\frac{v_\varphi}{v_\varphi^*}\right)^2}, \quad (1)$$

where $\eta(0)$ is the damping coefficient in the limit $v_\varphi \rightarrow 0$ and v_φ^* a critical velocity given by

$$v_\varphi^{*2} = \frac{D(14\zeta(3))^{1/2} \left(1 - \frac{T}{T_c}\right)^{1/2}}{\pi \tau_{in}}. \quad (2)$$

* Corresponding author.

Here D is the quasiparticle diffusion coefficient ($D = v_F l/3$, v_F is the Fermi velocity, l the electron mean free path); $\zeta(3)$ is the Riemann zeta function of 3, and τ_{in} the inelastic quasiparticle scattering time. At the velocity v_φ^* the damping force ηv_φ reaches a maximum, and at the corresponding voltage

$$V^* = -(v_\varphi^* \times B)L \quad (3)$$

the VIC displays a sharp kink which can be detected easily. Here B is the magnetic-flux density and L the sample length between the voltage contacts. The measurement of V^* and, hence, of v_φ^* yields important information on the inelastic scattering time τ_{in} .

The LO theory [3] and the results we have outlined above are valid near the critical temperature T_c . In this theory it is further assumed that the nonequilibrium distribution of the quasiparticles extends uniformly over the whole superconductor volume. This latter assumption is well satisfied as long as the distance $v_\varphi^* \tau_{in}$ is larger than about the intervortex distance a . In this case according to LO [3] the critical velocity v_φ^* is independent of the magnetic field, in agreement with our results reported earlier [1,2].

In Section 2 we describe experiments performed at low magnetic fields showing a characteristic magnetic-field dependence of v_φ^* . Section 3 deals with the investigation of the upper magnetic field limit up to which the electronic instability can be observed.

2. Regime of low magnetic fields

In the following we report on a characteristic magnetic-field dependence of v_φ^* observed at low magnetic fields. Apparently, there is a cross-over from the regime where $v_\varphi^* = v_{\varphi 0}^*$ independent of magnetic field to another regime where v_φ^* increases with decreasing magnetic field. The important length scale for this cross-over is the intervortex distance. Therefore, we expect this cross-over when

$$v_{\varphi 0}^* \tau_{in} = af(T), \quad (4)$$

where $f(T)$ is a numerical factor of order 1, which may be temperature dependent. If the magnetic field is reduced below the value where Eq. (4) is satisfied, the distance $v_{\varphi 0}^* \tau_{in}$ becomes too small, and the

quasiparticle distribution shows a strong spatial inhomogeneity with portions of the superconducting phase still displaying the quasiparticle equilibrium distribution. However, at such low magnetic fields spatial homogeneity of the quasiparticle distribution (assumed in the LO theory) can be recovered if v_φ^* increases accordingly. If we ignore the numerical factor $f(T)$ for the moment, and take into account that the inelastic scattering time has been found to increase strongly with decreasing temperature [1,2], we expect that the cross-over condition of Eq. (4) is shifted to lower magnetic fields with decreasing temperature. However, the quasiparticle distribution is governed by the superconducting energy gap which strongly increases with decreasing temperature. In this way a temperature-dependent energy scale is introduced into the problem of the nonequilibrium quasiparticle distribution which we describe by the empirical function $f(T)$ in Eq. (4). Qualitatively we expect $f(T)$ to decrease with increasing temperature, due to the correlation with the superconducting energy gap.

For the triangular vortex lattice we have

$$B = \frac{2}{\sqrt{3}} \frac{\varphi_0}{a^2}. \quad (5)$$

From Eq. (4) at sufficiently low fields we then expect the relation

$$v_\varphi^* = \left(\frac{2}{\sqrt{3}} \right)^{1/2} \left(\frac{\varphi_0}{B} \right)^{1/2} \frac{f(T)}{\tau_{in}} \quad (6)$$

In the following we show that this expectation is, indeed, experimentally observed.

Our experiments were performed along the lines described in Refs. [1] and [2], and we refer to these references for details. As before, the samples were thin films of epitaxial c -axis oriented $\text{YBa}_2\text{Cu}_3\text{O}_{7-\delta}$ deposited on single-crystalline MgO substrates by laser ablation. Microfabrication of the four-point sample geometry was performed by standard photolithography. Current and voltage leads were attached via silver contact pads as large as $2 \times 2 \text{ mm}^2$ in area. The length (between voltage leads) and width of the sample films was typically $200 \mu\text{m}$ and $20 \mu\text{m}$, respectively. The film thickness ranged between 60 and 150 nm. A magnetic field could be applied parallel to the c -axis. The samples studied

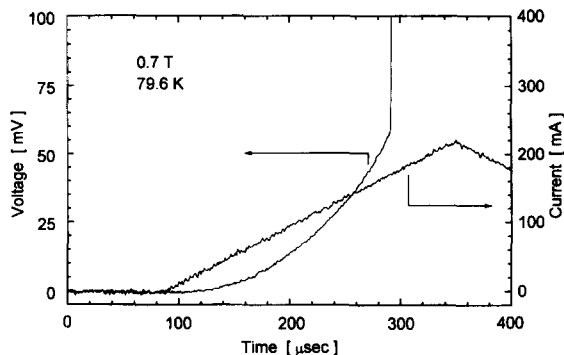


Fig. 1. Applied current and voltage vs. time for a single triangular current pulse ($T = 79.6$ K, $B = 0.7$ T).

had a sharp resistive transition within typically 2 K and zero-resistance critical temperature T_{c0} of 90 K. At 100 K the resistivity was 70–80 $\mu\Omega$ cm. For a detailed discussion regarding the elimination of Joule heating effects in our experiments we refer to Ref. [1]. All VIC's were measured using the rapid single-pulse technique of our previous experiments [1]: the current was swept up and down in a single triangular pulse, and the voltage was recorded simultaneously. The timescale for an upsweep was typically 0.3–1 ms. We have studied four samples all showing similar results.

In Fig. 1 we show typical experimental curves of the applied current I and the voltage V measured during a single pulse and plotted versus time. At $V = 58.6$ mV the temporal dependence of the voltage abruptly changes its slope turning into a nearly vertical branch. Note that the triangular current pulse slightly extends beyond this point, before the down-sweep of the current begins. The voltage $V = 58.6$ mV is interpreted as the flux-flow voltage V^* , corresponding to the critical velocity v_ϕ^* according to Eq. (3). A plot of the critical velocity v_ϕ^* versus magnetic field B (applied parallel to the c -axis) is presented in Fig. 2 for different temperatures. At high magnetic fields v_ϕ^* is seen to become field independent. It is this high-field regime where our previous results have been obtained [1,2], and our present data exactly confirm these earlier results. As an example in the inset of Fig. 2 we show the inelastic quasiparticle scattering rate τ_{in}^{-1} obtained using Eq. (2) and plotted versus temperature for sample I. However,

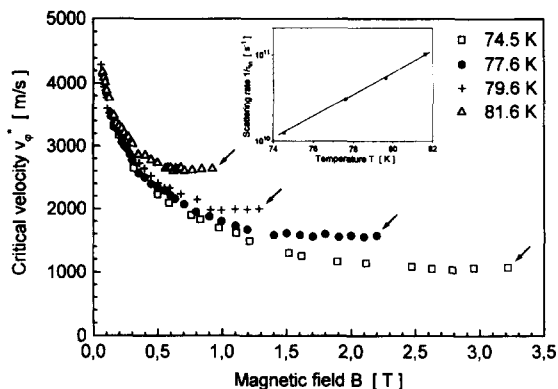


Fig. 2. Critical vortex velocity v_ϕ^* vs. magnetic field for different temperatures. The arrows mark the data points for the highest field at which the kink in the VIC was still observable. The inset shows the inelastic quasiparticle scattering rate τ_{in}^{-1} vs. temperature.

from Fig. 2 we see that at low magnetic field v_ϕ^* increases with decreasing B .

In view of our arguments leading to Eq. (6), in Fig. 3 we show typical curves of v_ϕ^* plotted versus $B^{-1/2}$. Whereas at high magnetic fields the data display the field-independent behavior discussed previously [1,2], the cross-over to the proportionality

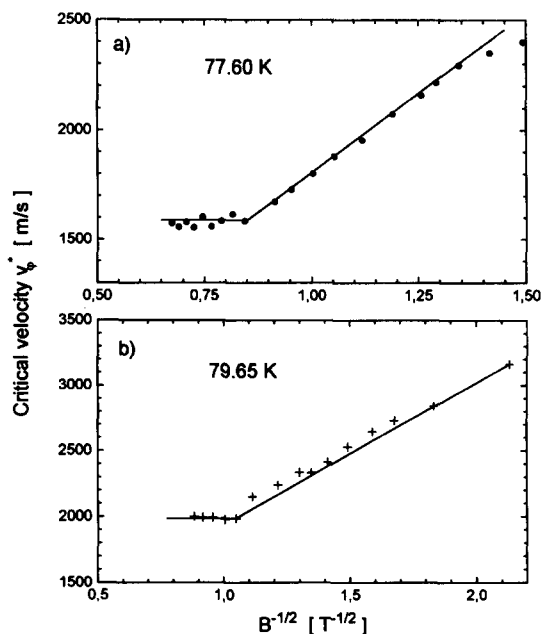


Fig. 3. Critical vortex velocity v_ϕ^* vs. $B^{-1/2}$ for two temperatures.

between v_φ^* and $B^{-1/2}$, expected from Eq. (6), can clearly be seen. In the following we discuss the temperature dependence of the magnetic field B^{**} , where the cross-over takes place, and of the slope of the straight lines such as shown in Fig. 3 for the regime of low magnetic fields. From both quantities the function $f(T)$ can be determined, according to Eqs. (4) and (6), respectively.

The values of $f(T)$ obtained for sample I from the slope of the straight lines found at low magnetic fields by plotting v_φ^* versus $B^{-1/2}$ (see Fig. 3) are shown in Fig. 4. These values were calculated using Eq. (6). Here the inelastic scattering time τ_{in} was taken from the magnetic-field independent values of v_φ^* measured at high fields and using Eq. (2) (see inset of Fig. 2). Furthermore, we have determined the cross-over field B^{**} from the intersection of the straight lines approximating our results on v_φ^* at low and high magnetic fields in plots such as shown in Fig. 3. From this cross-over field $f(T)$ has been calculated again using Eq. (4) and the same values of τ_{in} as before. This second set of $f(T)$ values is also plotted in Fig. 4. We see that both values of $f(T)$ agree reasonably with each other, indicating consistency between Eqs. (4) and (6). In the temperature range shown, with increasing temperature $f(T)$ decreases from above 1.0 to below 1.0. We have performed the same analysis with sample II yielding identical results.

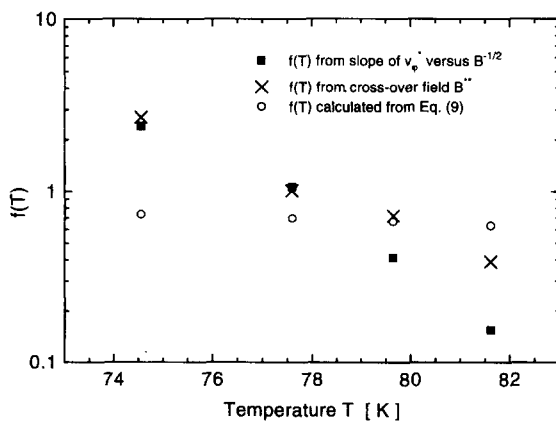


Fig. 4. Numerical factor $f(T)$ defined in Eq. (4) (crosses) and Eq. (6) (squares) vs. temperature. The open circles are calculated from Eq. (9).

We have based our discussion of the regime of low magnetic fields on the simple relation (4), yielding a qualitative understanding of our observations. In the following we extend our analysis by considering the inelastic scattering length $l_e = (D\tau_{in})^{1/2}$ and by replacing Eq. (4) with the condition

$$l_e = (D\tau_{in})^{1/2} = a. \quad (7)$$

The inelastic scattering length l_e is the length scale over which the quasiparticle excitations decay during current injection into a superconductor across an N/S boundary (electric-field penetration depth) [4]. Inserting D from Eq. (2) into Eq. (7) we obtain

$$v_\varphi^* \tau_{in} = a \frac{(14\zeta(3))^{1/4}}{\pi^{1/2}} \left(1 - \frac{T}{T_c}\right)^{1/4}. \quad (8)$$

Hence, for the function $f(T)$ of Eq. (4) we find

$$f(T) = \frac{(14\zeta(3))^{1/4}}{\pi^{1/2}} \left(1 - \frac{T}{T_c}\right)^{1/4}. \quad (9)$$

Some values of $f(T)$ calculated from Eq. (9) are also shown in Fig. 4. These values are not much different than our experimental results for $f(T)$. Furthermore, their temperature dependence is in the same direction but weaker than that of the experimental values.

3. Regime of high magnetic fields

Having dealt with the behavior at low magnetic fields, we next turn to the regime of high magnetic fields. The distinct kink in the VIC's associated with the electronic instability at high vortex velocities could be observed only up to a maximum field value B_{max} , which increased with decreasing temperature. In Fig. 2 the values B_{max} are reached at the magnetic fields where the horizontal parts of the curves terminate on the high-field end. The corresponding data points are marked by the arrows. The existence of this upper field B_{max} , above which the instability and the discontinuity in the slope of the VIC's disappear, can be qualitatively understood by noting that the flux-flow resistivity ρ_f cannot exceed the normal-state resistivity ρ_n . On the other hand, if the field values B_{max} have been found, from the electric field $|E_{max}| = v_\varphi^* B_{max}$, together with the current

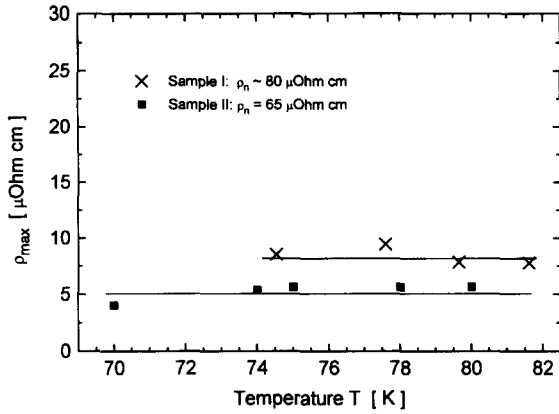


Fig. 5. Maximum resistivity ρ_{\max} from Eq. (10) corresponding to the maximum field B_{\max} at which the kink in the VIC was still observable vs. temperature for two samples.

density j , the corresponding electric resistivity

$$\rho_{\max} = \frac{v_{\varphi}^* B_{\max}}{j} \quad (10)$$

can be calculated. In Fig. 5 the values of ρ_{\max} found in this way are plotted versus temperature for samples I and II. It is interesting that for both samples ρ_{\max} is independent of temperature and amounts to about 10% of the normal-state resistivity. This value $\rho_{\max} \approx 0.1\rho_n$ is likely due to the fact that at this resistivity the discontinuity in the slope of the VIC starts to become smeared out by fluctuations, since the latter dominate the resistivity in the mixed state above about $0.5\rho_n$ [5].

4. Summary

In summary, we have shown that the critical vortex velocity v_{φ}^* , resulting in the electronic instability predicted by Larkin and Ovchinnikov, displays a cross-over effect from magnetic-field independent behavior at high fields to a distinct magnetic-field

dependence at low fields. Apparently, this cross-over is due to the requirement (assumed in the LO theory) that the nonequilibrium quasiparticle distribution is spatially homogeneous in the superconducting phase. As a consequence the distance $v_{\varphi}^* \tau_{\text{in}}$ cannot become smaller than the intervortex distance a . The distance $v_{\varphi}^* \tau_{\text{in}}$ is closely related to the inelastic scattering length of the quasiparticles. Hence, at low magnetic fields one expects the proportionality $v_{\varphi}^* \sim B^{-1/2} \tau_{\text{in}}^{-1}$. This expected behavior including the value of the cross-over magnetic field B^{**} are well confirmed by our measurements. An upper limit of the magnetic field, at which the electronic flux-flow instability can be observed, is reached when the resistivity starts to become influenced appreciably by fluctuations.

Acknowledgements

Financial support of this work by the Deutsche Forschungsgemeinschaft and clarifying discussions with Yu.N. Ovchinnikov are gratefully acknowledged. S.G. Doettinger was supported by the Studienstiftung Gerhard Rösch. S. Kittelberger and S. Simanowski provided technical assistance.

References

- [1] S.G. Doettinger, R.P. Huebener, R. Gerdemann, A. Kühle, S. Anders, T.G. Träuble and J.C. Villegier, Phys. Rev. Lett. 73 (1994) 1691.
- [2] S.G. Doettinger, R.P. Huebener, R. Gerdemann, A. Kühle, S. Anders, T.G. Träuble and J.C. Villegier, Physica C 235–240 (1994) 3179.
- [3] A.I. Larkin and Yu.N. Ovchinnikov, Zh. Eksp. Teor. Fiz. 68 (1975) 1915 [Sov. Phys. JETP 41 (1976) 960].
- [4] Nonequilibrium Superconductivity, Phonons, and Kapitza Boundaries, ed. K.E. Gray (Plenum, New York, 1981).
- [5] U. Welp, S. Fleshler, W.K. Kwok, R.A. Klemm, V.M. Vinokur, J. Downey, B. Veal and G.W. Crabtree, Phys. Rev. Lett. 67 (1991) 3180.